

9-2013

## KSHV encoded Rta induces cell cycle arrest

Pankaj Kumar

*University of Nebraska- Lincoln*

Charles Wood

*University of Nebraska- Lincoln, cwood1@unl.edu*

Follow this and additional works at: <http://digitalcommons.unl.edu/virologypub>

---

Kumar, Pankaj and Wood, Charles, "KSHV encoded Rta induces cell cycle arrest" (2013). *Virology Papers*. 250.  
<http://digitalcommons.unl.edu/virologypub/250>

This Article is brought to you for free and open access by the Virology, Nebraska Center for at DigitalCommons@University of Nebraska - Lincoln. It has been accepted for inclusion in Virology Papers by an authorized administrator of DigitalCommons@University of Nebraska - Lincoln.

1 **Kaposi's Sarcoma**-associated Herpesvirus Transactivator Rta Induces Cell Cycle Arrest in

2 G0/G1 Phase by Stabilizing and Promoting Nuclear Localization of p27<sup>kip</sup>

3

4 Running Title: KSHV encoded Rta induces cell cycle arrest

5

6 Pankaj Kumar and Charles Wood#

7 Nebraska Center for Virology and the School of Biological Sciences, University of Nebraska-

8 Lincoln, Lincoln NE 68583

9

10 Word Count

11 Abstract: 233

12 Text: 5958

13

14 Correspondent Footnote

15 102C Morrison Center

16 4240 Fair Street

17 University of Nebraska Lincoln

18 Lincoln NE 68583

19 USA

20 cwood1@unl.edu

21 Abstract

22 The Kaposi's sarcoma-associated herpesvirus (KSHV) encoded immediate early gene, replication  
23 and transcription activator (K-Rta) is a key viral protein that serves as the master regulator for  
24 viral lytic replication. In this study, we investigated the role of K-Rta in cell cycle regulation and  
25 found that the expression of K-Rta in doxycycline (Dox)-inducible BJAB cells induced cell cycle  
26 arrest in G0/G1 phase. Western blot analysis of key cell cycle regulators revealed that K-Rta-  
27 mediated cell cycle arrest was associated with a decrease in Cyclin A and phosphorylated Rb  
28 (pS807/ pS811) protein levels, both markers of S phase progression and an increase in protein  
29 levels for p27, a cyclin-dependent kinase inhibitor. Further, we found that K-Rta does not affect  
30 the transcription of p27 but regulates p27 at the post-translational level by inhibiting its  
31 proteosomal degradation. Immunofluorescence staining and cell fractionation experiments  
32 revealed largely nuclear compartmentalization of p27 in K-Rta expressing cells demonstrating  
33 that K-Rta not only stabilizes p27 but also modulates its cellular localization. Finally, shRNA  
34 knockdown of p27 significantly abrogates cell cycle arrest in K-Rta expressing cells supporting  
35 its key role in K-Rta mediated cell cycle arrest. Our findings are consistent with previous studies  
36 which showed that expression of immediate early genes of several herpes viruses including HSV,  
37 EBV and CMV results in cell cycle arrest at the G0/G1 phase, possibly to avoid competition of  
38 resources needed for host cell replication during the S phase.

## 39 Introduction

40 Kaposi's sarcoma-associated herpesvirus (KSHV), also known as Human herpesvirus-8  
41 (HHV-8) is a member of gammaherpesvirus family that includes Epstein Barr Virus (EBV),  
42 Herpesvirus saimiri (HVS) and Murid herpesvirus 68 (MHV 68) (1). KSHV is the etiological  
43 agent of Kaposi's sarcoma (KS), the most common tumor associated with HIV infection and for  
44 at least two other malignancies, pleural effusion lymphoma (PEL) and multicentric Castleman's  
45 disease (MCD) (2-4). Like all herpesviruses, the life cycle of KSHV consists of latent and lytic  
46 phases. The latent phase is characterized by a restricted pattern of viral gene expression that  
47 facilitates the evasion of immune surveillance and the establishment of lifelong persistent  
48 infection. The lytic phase drives the replication cycle and a majority of the viral genes are  
49 expressed in this phase. This phase mainly allows for the spread of the virus in the infected  
50 individual. A growing body of research suggests that both latent and lytic replication phases play  
51 an important role in the pathogenesis of KS (5).

52 The transition from latency to lytic replication is controlled by the KSHV replication and  
53 transcription activator (K-Rta) gene, an immediately early gene encoded by open reading frame  
54 50 (ORF50). K-Rta expression has been found to be essential and sufficient to trigger lytic  
55 replication by activating the lytic gene expression cascade (6-8). Genetic knockout of K-Rta  
56 resulted in a null phenotype in viral DNA synthesis and in virus production (9). K-Rta is a 691-  
57 amino acid (aa) long transcriptional factor that contains an N-terminal DNA-binding domain and  
58 a C-terminal activation domain. K-Rta can trigger KSHV lytic reactivation via transcriptional  
59 activation of a number of viral lytic promoters, by either binding directly to the promoter DNA  
60 or indirectly via interaction with cellular DNA binding proteins (10-15).

61 There is a complex interplay between herpesvirus lytic replication and host cell cycle  
62 arrest. Previous studies investigating the role of cell cycle in herpesvirus lytic replication

63 suggested that host cell cycle arrest precedes the induction of lytic cycle and essentially  
64 determines whether immediate early gene expression is initiated or not (16). However, current  
65 research increasingly support the idea that cell cycle arrest follows lytic cycle induction and is a  
66 direct consequence of immediate early gene expression (17-19). It is hypothesized that arresting  
67 cells during early lytic replication may be an evolutionary common strategy employed by  
68 herpesviruses to avoid competition of resources required for viral DNA replication with the host  
69 in the S phase, or it may serve to prevent premature apoptosis during lytic replication (20). This  
70 is in contrast to small DNA viruses, especially those lacking their own polymerase like SV40 and  
71 adenoviruses which actively drive host cells into S phase of the cell cycle in order to replicate  
72 their genome at the same time with host DNA synthesis. Arresting cell growth early during  
73 infection/reactivation may also be a strategy to avoid being killed by cytotoxic T cells as it has  
74 been reported that non-cycling cells are refractory to killing by cytotoxic T cells (21).

75 To date, several herpesvirus-encoded proteins have been identified that participate in  
76 arresting host cell growth. These proteins are either virion components and/or immediate early  
77 (IE) transcriptional factors. For example, the IE product of herpes simplex virus, ICPO has been  
78 found to arrest cell cycle in G1 phase by both p53 mediated and p53 independent pathways (22,  
79 23) . In the case of EBV, immediate early product, Zta can induce host cell cycle arrest by  
80 stabilizing p53 and p27, and also through repressing the expression of c-myc (24, 25).  
81 Furthermore it has been shown that Zta may cooperate with host transcriptional factor C/EBP to  
82 upregulate p21, which in turn results in cell cycle arrest (26).

83 Among the characterized early genes of KSHV, K8 or K-bZIP protein, a functional  
84 homologue of EBV's immediate early Zta protein was shown to arrest PEL cells in G1 phase  
85 during lytic cycle by up regulating C/EBP and p21 proteins (27). K8 was also found to inhibit  
86 kinase activities of CDK2 by directly binding through its bZIP domain (17). However the role of

87 KSHV encoded ORF50/K-Rta, one of the first genes transcribed and the central regulator for the  
88 initiation of lytic replication cycle, in cell cycle regulation has not been evaluated. In the present  
89 study, we demonstrated that K-Rta induces cell cycle arrest in an inducible BJAB cell model and  
90 this growth arrest is mediated by elevated levels of p27, a central cyclin-dependent kinase  
91 inhibitor (CDKI). Our results shed new light on the biological function of K-Rta as a key cell  
92 cycle regulator early on during viral reactivation, in addition to being a transcriptional regulator.

## 93 Materials and Methods

94 Cell culture plasmids and transfection. 293T cells, 293 based doxycycline-inducible K-Rta  
95 cell line (TREx293Rta) (provided Dr Yoshihiro Izumiya, University of California at Davis,  
96 California) and Vero cells were cultured in Dulbecco's modified Eagle's medium (DMEM;  
97 Invitrogen, Carlsbad CA) supplemented with 10% fetal bovine serum (FBS; HyClone, Logan,  
98 UT) and 100 µg/ml penicillin-streptomycin (Mediatech). DG75 is an EBV-negative Burkitt's  
99 lymphoma (BL) derived B-cell line (provided by Dr. Luwen Zhang, University of Nebraska-  
100 Lincoln, Lincoln NE). It was grown in RPMI 1640 medium (Gibco BRL) supplemented with  
101 10% FBS and 100 µg/ml penicillin-streptomycin. TRExBJABRta and TRExBJAB cells are  
102 BJAB (EBV and KSHV negative B-cell line) derived cell lines with or without doxycycline-  
103 inducible K-Rta gene. They were provided by Dr Jae Jung (University of Southern California,  
104 Los Angeles, CA) (28) and were grown in RPMI 1640 medium supplemented with 10% FBS,  
105 100 µg/ml penicillin-streptomycin and 200 µg/ml of hygromycin B. KSHV-positive and EBV-  
106 negative B cell lines, BC3 cells (ATCC, USA) and Cro6 (29) (provided by Dr. Luwen Zhang,  
107 University of Nebraska-Lincoln, Lincoln NE) were grown in RPMI 1640 medium (ATCC, USA)  
108 supplemented with 20% FBS and 100 µg/ml penicillin-streptomycin. Human Microvascular  
109 Endothelial Cells (HMVEC) cells were grown in endothelial basal medium-2 (EBM-2) (Lonza,  
110 Boston, MA) supplemented with 10% fetal bovine serum (FBS), 100 µg/ml penicillin-  
111 streptomycin, 0.01 µg/ml epidermal growth factor, and 1 µg/ml hydrocortisone (30). All cultures  
112 were incubated at 37°C with 5% CO<sub>2</sub>.

113 K-Rta expression plasmid (pCMVtagORF50), which encodes Flag-tagged full length Rta  
114 and pCMVtagORF50 (1-527), which encodes truncated K-Rta (amino acid 1 to 527), were  
115 described previously (31). The transfection of 293T cells and Vero cells was carried out using  
116 Lipofectamine 2000 (Invitrogen) or Fugene 6 (Promega) according to the manufacturer's

117 recommendations. The transfection of DG75 was carried out using the nucleofection protocol  
118 according to the manufacturer's protocols (Solution V and program O-006, Amaxa Biosystems).  
119 Cell Cycle analysis. Cell cycle profiles were analyzed by flow cytometry with standard  
120 propidium iodide (PI) staining methods (32). Asynchronized and synchronized cells were  
121 harvested at given time points, washed once with PBS and fixed in 70% ethanol at -20°C. After  
122 collection of all time points, the cells were washed with PBS twice and were resuspended in PBS  
123 containing PI (Roche) at a final concentration of 10 µg/ml and RNase A (20 µg/ml). The samples  
124 were kept at RT for 30 min in dark and 20,000 events per sample were acquired using FACS  
125 Calibur flow cytometer (BD Biosciences). The data was analyzed using Modfit LT version 2.0  
126 software (Verity Software House Inc.).

127 RNA extraction and RT-PCR. Total cellular RNA was extracted using an RNeasy kit  
128 (QIAGEN) according to the manufacturer's procedure. RNA samples were digested with DNase  
129 (Invitrogen) to remove any residual DNA. Total RNA (2 µg) was used for reverse transcription  
130 (RT) using oligo(dT) as primers and Superscript II reverse transcriptase kit (Invitrogen, Inc.,  
131 Carlsbad, CA) according to the manufacturer's instructions. The primers used for the mRNA  
132 quantitation were p27 (F) 5-CGTCAAACGTAAACAGCTCG-3 and p27 (R)- 5-  
133 CATTCCATGAAGTCAGCGAT-3, ORF50 (F)- 5-CAAACCCCATCCCAACAT-3 and ORF50  
134 (R)- 5-AGTAATCACGGCCCCTT-3, GAPDH (F) - 5-CCATGGAGAAGGCTGGGG-3 and  
135 GAPDH (R)- 5-CAAAGTTGTCATGGATGACC-3. These target genes were amplified using  
136 the iQ SYBER green real time master mix (BioRad) in a BioRad iCyclerIQ thermocycler. All  
137 reactions were performed in triplicate using the following conditions: 50°C for 2 min, 95°C for  
138 10 min, 40 cycles of 95°C for 15 sec and 60°C for 1 min. Melting-curve data for all the samples  
139 were obtained to ensure specific amplification. All reactions were performed in triplicate and  
140 included no-template controls for each gene. The experiments were repeated 2 times using



141 samples in triplicate. Relative gene expression was calculated using delta-delta-CT method (33).  
142 For calculating relative mRNA levels, the CT (threshold cycle) value of each gene was  
143 normalized to the CT value of GAPDH, and the normalized CT values from samples were  
144 compared to those of the control samples (untreated).

145 Immunoprecipitation and immunoblot analysis. Total cell lysates for immunoprecipitation  
146 and western blotting were prepared in radioimmunoprecipitation assay buffer (RIPA) (50 mM  
147 Tris-HCl (pH 8.0), 150 mM NaCl, 1 mM EDTA, 1% NP-40) supplemented with protease and  
148 phosphatase inhibitor cocktail (Pierce). The lysates were kept in ice for 30 min with occasional  
149 vortexing. Finally, the lysates were centrifuged for 15 min at 13,000 x g at 4°C and the  
150 supernatant was collected. Cytosolic and nuclear proteins were extracted from TRExBJABRta  
151 cells using Sigma-CellLytic™ NuCLEAR™ Extraction Kit using manufacturer's protocol. The  
152 protein concentration was measured using a BCA protein kit (Pierce, Rockford, IL). For  
153 immunoprecipitation, equal amount of lysate from each treatment was precleared with 20 µl of  
154 Protein A/G Sepharose (1hr, 4°C). Five percent of the precleared lysate was saved as input  
155 control and total amount of p27 was captured by incubating with 2 µg of anti-p27 (SC-1641;  
156 Santa Cruz) antibody overnight at 4°C. Immune complexes were captured with 30 µl of a 1:1  
157 mixture of Protein-A and Protein-G Sepharose beads (Pierce, Rockford, IL) for 2 hrs. The beads  
158 were then pelleted and washed three times with ice-cold RIPA buffer. The immunoprecipitated  
159 proteins were eluted by heating in 2X sample buffer and subjected to immunoblotting.

160 For immunoblotting, equal amounts of total proteins (40 µg) were separated by sodium  
161 dodecyl sulfate polyacrylamide gel electrophoresis (SDS-PAGE) and subsequently transferred to  
162 nitrocellulose membrane using standard methods. After blocking with 5% non-fat dry milk in  
163 Tris-buffered saline (TBS) (20 mM Tris pH-7.4, 137 mM NaCl) containing 0.01% Tween-20  
164 (TBST) for 1 hr, the membrane was incubated with primary antibody overnight at 4°C.

165 Following washing with TBST three times, the membrane was incubated with horse peroxidase  
166 conjugated goat anti-rabbit/mouse secondary antibody (1:10000, Pierce) or infrared-tagged  
167 secondary antibodies (1:10000, Licor Inc., Lincoln, NE) for 30 min. Antibody binding was  
168 detected using SuperSignal West Dura Extended Duration Substrate kit (Pierce) or using an  
169 Odyssey imager. Image analysis and quantification of immunoreactive bands was performed  
170 using the Odyssey Infrared Imaging System application software (LiCor Inc., Lincoln, NE) or  
171 NIH ImageJ software.

172 Following antibodies were used in the present study: anti-rabbit K-Rta antibody was a  
173 kind gift from Dr Izumiya (UC Davis, California) and was used at a dilution of 1:5000. The anti-  
174 rabbit p27 (SC-528), anti-mouse p27 (SC-1641), anti-rabbit p21 (SC-397), anti-rabbit Rb  
175 (pS807/pS811) (BD558389), anti-rabbit Cyclin A (SC-751), anti-mouse GAPDH (SC-32233),  
176 anti-mouse Ub (SC-8017), anti-rabbit Skp2 (H-435), anti pp27-T187 (Ab75908 ), anti-mouse  
177 TATA binding protein (Ab818), anti-mouse  $\alpha$  tubulin (SC-5286) were used at 1:1000 dilution in  
178 TBST.

179 Protein stability test. Exponentially growing TRExBJABRta cells were cultured in the presence  
180 of doxycycline (DOX) for 24 hrs. DOX treated and untreated cells were treated with 50  $\mu$ g/ml  
181 cyclohexamide (CHX) (Sigma-Aldrich, St. Louis, MO). The cells were harvested at indicated  
182 time points after CHX treatment and cell lysates were subjected to Western blot analysis. Band  
183 intensities were quantitated using Odyssey 3.0 software provided by Odyssey imager (LiCor  
184 Inc., Lincoln, NE) and the half-life of p27 protein was calculated from the slope of the curve.  
185 Immunofluorescence assay. TRExBJABRta cells were treated with doxycycline for 48 hrs. The  
186 cells were fixed with 4% paraformaldehyde for 20 min, permeabilized with 0.2% Triton X-100  
187 in phosphate buffered saline (PBS) for 10 minutes, and blocked for 30 min with 2% bovine  
188 serum albumin (BSA) in PBS at room temperature (RT). After incubation with primary

189 antibodies [anti-p27 mouse monoclonal (BD) and anti-rabbit K-Rta] both at 1:250 dilution in 2%  
190 BSA for 2 hrs at RT, the cells were incubated with anti-mouse Alexa-Fluor-488 and anti-rabbit  
191 Alexa-Fluor-647 conjugated secondary antibodies (1:1000) for 1 hour at RT. This was followed  
192 by three washes with PBS. The last wash contained 4',6-diamidino-2-phenylindole (DAPI)  
193 (Calbiochem) to counterstain nuclei. The localization of K-Rta/p27 and DAPI stained nuclei  
194 were visualized by confocal microscopy.

195 Lentivirus-based short hairpin RNAs (shRNA) knockdown of p27. To establish p27  
196 knockdown cell line, plasmids encoding p27 shRNA (1 and 2) and scrambled negative control  
197 shRNA (1 and 2) were purchased from Origene and were transfected into TReXBJABRta cells  
198 using the Nucleofector kit T from Lonza (Walkersville, MD) according to the manufacturer's  
199 procedure (Program- G-016). The transfected cells were selected with puromycin (1  $\mu$ g/ml) for 3  
200 weeks.

201 Lentivirus vector expressing full length K-Rta, virus production and transduction of  
202 HMVEC cells. To generate a lentiviral vector expressing KSHV full length Rta, the coding  
203 sequence was cloned into pLVX-AcGFP1 (Clontech). The VSV-G-pseudotyped lentiviral  
204 particles were produced by transient cotransfection of 293T cells as described (34). Briefly, 5-6  
205  $\times 10^6$  HEK293T cells were co-transfected with 18  $\mu$ g of K-Rta expressing transfer vector (pLVX-  
206 Rta), 12  $\mu$ g packaging vector psPAX2, and 6  $\mu$ g of envelope vector pHEF-VSVG per 10 cm  
207 diameter plate at a 3:2:1 mass ratio by using standard calcium phosphate co-precipitation  
208 method. Eight hours post-transfection the media was replaced with DMEM supplemented with  
209 10% FBS. The medium containing the virus was harvested 48 hours post-transfection, filtered  
210 through 0.45  $\mu$ m pore filter and concentrated by ultracentrifugation at 4°C for 2 hrs at 25,000  
211 rpm with T-865 rotor (Sorvall). Pellets were gently resuspended in DMEM and kept over-night  
212 at 4°C. The viral titers of concentrated pseudotyped lentiviruses were determined by transducing

213  $3 \times 10^5$  293T cells seeded in one well of a 6-well plate in 4 ml of medium containing 8  $\mu\text{g/ml}$  of  
214 polybrene (Sigma). The media was replaced after 6 hrs. After 48 hours the number of cells  
215 expressing GFP was determined using flow cytometry. The viral titers were calculated using the  
216 formula:  $N \times M / V$  where N is the number of target cells used for infection, M is % GFP  
217 expressing cells, and V is the volume of concentrated virus used in ml.  
218 Statistical Analysis. All data analysis was done using SPSS software (v11). Comparison of  
219 mean number of cells was done using Student's t-test. All p-values  $\leq 0.05$  were considered  
220 significant.

## 221 Results

222 Expression of K-Rta induces cell cycle arrest in G1 phase: Earlier investigations have  
223 reported that TPA-induced reactivation of KSHV results in cell cycle arrest in G1 phase of the  
224 treated cells and implicated early-lytic gene product K-bZIP for the induction of cell cycle arrest  
225 (17). Indeed TPA treatment of asynchronously growing BC3 cells (KSHV positive latent B-cell  
226 line) resulted in a marked increase of cells in the G1 fraction at 24 hrs after treatment, from 37%  
227 (before treatment) to 56.5%. This increase in proportion of cells arrested in G1 phase was also  
228 noted after TPA treatment of another KSHV positive latent B-cell line, Cro6, with a significant  
229 increase from 55.6% (before treatment) to 70.5% at 24 hrs post treatment. However TPA  
230 induced G1 arrest was not observed in KSHV negative control B-cell line DG75, at 24 hrs post  
231 TPA treatment (Fig. 1). These results confirmed previous findings that KSHV lytic reactivation  
232 arrests naturally infected B cells in G1 phase.

233         Since G1 arrest is favored after lytic replication, we sought to investigate whether any  
234 other immediate early genes besides K-bZIP was involved in cell cycle arrest. We hypothesized  
235 that K-Rta being the central regulator of viral lytic cycle and one of the very first genes to be  
236 transcribed following reactivation may work in concert with K-bZIP to arrest cell cycle in G1  
237 phase. To investigate K-Rta's role in cell cycle regulation, we utilized TRExBJABRta cells in  
238 which myc-tagged full length K-Rta gene is integrated into the chromosomal DNA under the  
239 control of a tetracycline-inducible promoter. Asynchronously growing exponential cultures of  
240 TRExBJAB (Control) and TRExBJABRta were synchronized in G0/G1 phase by serum  
241 starvation. The cells were released from growth arrest with the addition of medium containing  
242 10% serum along with doxycycline. We then quantitated the fraction of cells in different phases  
243 of cell cycle by flow cytometry at 24, 48 and 72 hrs post Dox treatment for both TRExBJAB and  
244 TRExBJABRta cells. The fraction of cells arrested in G0/G1 phase after 24 hrs of serum

245 starvation treatment was about 53% for both cell lines. Serum starvation for extended time was  
246 avoided as it affected cell viability. The cell cycle profiles of both cell lines were similar  
247 following release from serum starvation without Dox treatment and showed enrichment of cells  
248 in S phase over time (Data not shown). Interestingly cell cycle profile clearly showed a  
249 significant increase in the number of cells arrested at G1 phase in TRExBJABRta cells compared  
250 to control TRExBJAB cells at 48 hrs ( $p=0.006$ ) and 72 hrs ( $p<0.001$ ) post Dox treatment (Fig.  
251 2A). In contrast, there were more cells in S phase for TRExBJAB cells after 48 and 72 hr of Dox  
252 treatment, demonstrating that doxycycline alone has little or no effect on cell cycle progression  
253 following the release of cell cycle arrest in the absence of K-Rta. A significant arrest in G1 phase  
254 was also noted for Dox treated TREx293Rta cells at 72 hrs post treatment compared to untreated  
255 cells ( $p <0.001$ ) (Fig. 2B) further supporting the data observed in BJAB cells. These results  
256 clearly show that the expression of K-Rta alone can induce cell cycle arrest in G1 phase.  
257 K-Rta expression led to a decrease in phosphorylated Rb and a parallel increase in p27<sup>kip1</sup>  
258 protein levels: To explore the underlying mechanism of K-Rta mediated cell cycle arrest, the  
259 expression kinetics of key cell cycle regulators were analyzed by western blotting. Whole cell  
260 lysates were prepared from Dox treated and untreated TRExBJAB and TRExBJABRta cells.  
261 First we investigated the phosphorylation status of Retinoblastoma (Rb) protein, a critical  
262 negative regulator of the cell cycle that undergoes differential phosphorylation during the cell  
263 cycle (35). In early G1 phase Rb is largely dephosphorylated and bound to E2F family of  
264 transcriptional factors, forming a repressor complex. However, upon phosphorylation by  
265 Cdk4/6/cyclin D complex during early G1 phase and further by Cdk2/cyclin E during late G1  
266 phase, Rb dissociates from E2F, thus activating the expression of proteins needed for S-phase  
267 entry and progression (35). We examined the status of Rb phosphorylation using an antibody that  
268 recognizes Rb phosphorylated at Ser807/Ser811. These sites are the target sites of Cdk4/6/cyclin

269 D complex during G1 phase. Induction of K-Rta in TRExBJABRta cells resulted in a significant  
270 decrease in the phosphorylated levels of Rb, most notably at 48 and 72 hrs post Dox treatment  
271 (Fig. 3A). The results were markedly different in Dox untreated TRExBJABRta, which  
272 displayed a significant increase in the levels of phosphorylated Rb in a time dependent manner  
273 that reached peak expression by 48 hrs, indicating that most of these cells were actively  
274 progressing through the cell cycle. In control TRExBJAB cells, the levels of phosphorylated Rb  
275 increased in a time dependent manner following release from cell cycle arrest, irrespective of  
276 Dox treatment suggesting that Dox treatment alone did not affect the normal cell cycle  
277 progression. Cyclin A is useful marker for S phase whose expression increases during cell cycle  
278 progression (36). Cyclin A expression in both cell lines with or without Dox treatment followed  
279 the expression kinetics similar to phosphorylated Rb.

280         Since the activities of G1 cyclin-CDK complexes are mainly regulated by Cip/Kip family  
281 of Cyclin dependent kinase inhibitors (CDKIs), we aimed to evaluate the expression profile of  
282 p21 and p27, two central regulators of cell cycle progression that inhibit a broad range of cyclin  
283 Cdk complexes. The levels of p27 significantly increased over time in Dox treated  
284 TRExBJABRta cells but the kinetics of p27 protein accumulation lagged by about 24 hrs  
285 following the expression of Rta in TRExBJABRta cells, reaching maximum levels at 48 hrs  
286 (~5X above background) whereas in untreated cells, p27 levels decreased in a time dependent  
287 manner. In TRExBJAB cells, the expression kinetics of p27 was similar in both Dox treated or  
288 untreated cells and was consistent with those described for cells entering S phase following cell  
289 cycle arrest in G1 phase. The levels of p21 remained largely unchanged during the course of  
290 experiment for both cell lines irrespective of Dox treatment. Since p21 is a direct transcriptional  
291 target of p53, we also investigated the expression levels of p53 and found no significant change  
292 in the relative levels of p53 in both cell lines with or without Dox treatment (data not shown).

293 These results demonstrated that K-Rta-mediated cell cycle arrest in BJAB cells does not involve  
294 p21 and is associated with a decrease in Rb phosphorylation and a parallel increase in p27 levels.

295 We also examined the expression of p27 in TPA treated BC3 cells and found that p27  
296 levels increased in a time dependent manner following reactivation (Figure 3B). This increase in  
297 p27 levels was not observed in TPA treated DG75 cells. Although this increase in p27 levels in  
298 TPA treated BC3 cells does not directly implicate K-Rta but it does show that cell cycle arrest  
299 during reactivation of KSHV from a latently infected B cell line is associated with an increase in  
300 p27 levels.

301 To ensure that K-Rta mediated up regulation of p27 in BJAB cell line was not a cell type  
302 specific effect, we transiently transfected or transduced K-Rta in DG75, Vero cells and HMVEC  
303 cells respectively and checked the levels of p27 at 36 hours post-transfection/transduction by  
304 western blotting (Figure 3C) while the cells were actively growing at log phase. We found  
305 increased levels of p27 in cells that were transfected or transduced with K-Rta compared to cells  
306 that were transfected/transduced with vector or control virus. These results suggest that increase  
307 in p27 levels following K-Rta expression is not unique to BJAB cells.

308 K-Rta does not affect p27 at the transcriptional level: Since K-Rta is a transcriptional factor  
309 and has the ability to regulate the expression of cellular genes (37); we investigated the  
310 possibility whether the increased level of p27 in K-Rta expressing cells is due to transcriptional  
311 up regulation of p27 by K-Rta. Real time PCR was carried out with RNA samples extracted from  
312 Dox treated and untreated cells. As shown in figure 4A, the level of p27 mRNA after  
313 normalization with GAPDH showed no significant difference before and after K-Rta induction.  
314 The data suggest that the up regulation of p27 in K-Rta expressing cells is not due to increased  
315 p27 mRNA expression. These results were also supported by increased p27 levels observed in  
316 cells transiently transfected with K-Rta lacking the transactivation domain, suggesting that K-Rta



317 is not directly acting on p27 at the transcriptional level or the ability of K-Rta to upregulate p27  
318 is independent of its transactivation function (Fig. 4B).

319 K-Rta expression results in stabilization of p27: Since p27 is mainly regulated at the post-  
320 translational level via the ubiquitin-proteasome pathway (38, 39), we examined the effect of K-  
321 Rta on the half-life of p27. Protein synthesis was blocked in K-Rta expressing BJAB cells by  
322 cycloheximide and p27 protein levels were quantitated at various time intervals by  
323 immunoblotting (Fig. 5A). As a control, we also followed p27 levels in Dox untreated  
324 TRExBJABRta cells. In control cells, the half-life of p27 was found to be approximately 4.1 hrs  
325 but in K-Rta expressing cells the half-life of p27 increased to approximately 7.3 hrs. The data  
326 suggest that upregulation of p27 in K-Rta expressing cells is most likely mediated by changes in  
327 protein stability. Next, we investigated the possibility whether reduced poly-ubiquitination of  
328 p27 in K-Rta expressing cells is responsible for increased levels of p27. Poly-ubiquitination of  
329 the p27 was assessed by immunoprecipitating p27 from Dox treated and untreated  
330 TRExBJABRta cells followed by immunoblotting (Fig. 5B). As expected, there was an increase  
331 in p27 levels in K-Rta expressing cells in both lysate and immunoprecipitated lanes, however we  
332 detected decreased levels of ubiquitinated p27 in Dox-treated TRExBJABRta cells as evidenced  
333 by a reduction of the smear of high molecular weight p27 bands as compared to the uninduced  
334 Dox lane. These results suggest that the expression of K-Rta increases p27 stability by inhibiting  
335 the poly-ubiquitination and subsequent proteasomal degradation.

336 K-Rta promotes nuclear localization of p27: The activity of p27 is also regulated by its  
337 subcellular localization as it shuttles between nucleus and cytoplasm during the cell cycle (40).  
338 p27 is exclusively nuclear during G0/G1 phase but is exported to the cytoplasm in response to  
339 proliferating signals. Since the subcellular localization of p27 is inherently linked to the  
340 regulation of p27 activity, we determined whether K-Rta is modulating the subcellular

341 localization of p27. The localization of endogenous p27 was investigated in Dox treated and  
342 untreated TRExBJABRta cells by indirect immunofluorescence assay. Figure 6A shows a  
343 representative field of immunostaining. As expected, intense staining suggesting higher p27  
344 expression levels were observed in most K-Rta expressing cells. Further, the staining for p27 was  
345 predominantly nuclear and colocalized with K-Rta. In most of the untreated TRExBJABRta  
346 cells, the staining for p27 was less intense and mostly diffuse. In order to confirm the effects of  
347 K-Rta on p27 localization observed in immunofluorescence assay, we performed cell  
348 fractionation to determine the levels of p27 in nuclear and cytosolic extracts of untreated and  
349 treated TRExBJABRta by western blot (Fig. 6B). We found a significant fraction of p27 in the  
350 nuclear extracts (normalized to the total p27 levels) of K-Rta expressing BJAB cells (43% vs.  
351 14%) compared to the control cells. These results demonstrate that in addition to increased  
352 stability of p27, modulation of the intracellular localization of p27 also occurred in K-Rta  
353 induced G1 arrest.

354 K-Rta induced cell cycle arrest coincides with down regulation of Skp2: Multiple  
355 degradation pathways that regulate p27 protein levels have been characterized in recent years  
356 (39). One of the best-understood pathways for degradation of p27 is mediated by SCF/Skp2  
357 complex in late G1 phase and early S phase (41). CDK2-dependent phosphorylation at T187  
358 targets p27 to SCF/ Skp2 complex for ubiquitin-dependent degradation (42). CDK2-dependent  
359 phosphorylation at T187 and binding of phosphorylated p27 to Skp2 are both considered rate-  
360 limiting steps for p27 ubiquitination and subsequent degradation (43, 44). We examined both  
361 these events to better define the mechanism of K-Rta mediated up regulation of p27. Figure 7  
362 shows the kinetics of Spk2 and p27 phosphorylated at T187 from Dox treated and untreated  
363 TRExBJABRta cells at various time intervals following release of cell cycle arrest. Skp2 levels  
364 decreased over time with kinetics that parallel increase in the levels of p27 in K-Rta expressing

365 cells. In Dox untreated TRExBJABRta cells, the kinetics was opposite with gradual  
366 accumulation of Skp2 over time. In K-Rta expressing cells, there was a decrease in the level of  
367 p27 phosphorylation at T187 and a parallel increase in the total p27 levels. However, in Dox  
368 untreated cells the level of phosphorylated p27 at T187 gradually increased over time with a  
369 parallel decrease in p27 levels as expected. These results suggest that K-Rta mediated up  
370 regulation of p27 is most likely a Skp2 dependent event and T187 is the key phosphorylation site  
371 targeted.

372 Knock down of p27 expression by shRNAs mitigates K-Rta induced cell cycle arrest. The  
373 data above strongly suggest that K-Rta induced cell cycle arrest involved impaired degradation  
374 of p27 by Skp2 resulting in accumulation of p27 in the nucleus. To conclusively prove that the  
375 observed accumulation of p27 had the causal effect on the cell cycle arrest or is directly  
376 responsible for K-Rta mediated cell cycle arrest, we knocked down p27 expression in  
377 TRExBJABRta cell line by stably expressing shRNAs against p27. Western blot analysis of Dox  
378 treated TRExBJABRta cell lines expressing shRNA against p27 showed efficient but incomplete  
379 knock down of p27 expression (~80% in both clones 1 and 2) (Fig. 8A). TRExBJABRta cell  
380 lines expressing control shRNAs (Clone 1 and 2) showed no significant reduction in the levels of  
381 p27 compared to the parent TRExBJABRta cell line. Next we quantitated cells in G1 phase from  
382 TRExBJABRta cells expressing these shRNAs after release from mitotic arrest and treatment  
383 with Dox. The results from FACS analysis showed that the down regulation of p27 by shRNA  
384 results in a significant decrease in K-Rta induced G1 arrest, ~60% in G1 phase compared to  
385 ~70% cells in G1 phase in parent TRExBJABRta cells or TRExBJABRta cells stably expressing  
386 control shRNAs (Fig. 8B). We did not observe total abrogation of cell cycle arrest in G1 phase in  
387 TRExBJABRta cells expressing shRNA against p27 but we noticed a significant decrease of  
388 cells in G1 phase compared to TRExBJABRta cells expressing control shRNA. The data suggest

389 that the accumulation of p27 observed in K-Rta expressing cells contributes to cell cycle arrest at  
390 G1.

## 391 Discussion

392 Our study demonstrates that KSHV encoded immediate early gene K-Rta induces cell  
393 cycle arrest in G0/G1 phase in an inducible B-cell line model. Consistent with G1 arrest, K-Rta  
394 mediated cell cycle arrest was associated with a decrease in the protein levels for cyclin A and  
395 phosphorylated Rb, both markers of S phase progression. Importantly, our results establish p27,  
396 a critical cyclin-dependent kinase inhibitor (CDKI) as a key player in K-Rta mediated cell cycle  
397 arrest. The central role of p27 in K-Rta mediated G1 arrest is supported by shRNA knockdown  
398 of p27, which significantly overrode the cell cycle arrest in K-Rta expressing cells. Since the  
399 knockdown of p27 did not completely abolish K-Rta mediated G1 arrest, we cannot exclude the  
400 possibility that K-Rta may also be functioning through other pathways that could contribute to  
401 cell cycle arrest.

402 Our finding that K-Rta arrests cells in G0/G1 phase is in general agreement with recent  
403 studies that investigated the role of EBV encoded Rta (E-Rta) in cell cycle regulation (18). The  
404 expression of inducible E-Rta in 293 and nasopharyngeal carcinoma (NPC) derived cells resulted  
405 in G1 arrest (18, 19) which was associated with elevated levels of p21 and p27. However, we did  
406 not notice any significant changes in the expression of p21 in K-Rta expressing cells. It is  
407 possible that E-Rta and K-Rta may have evolved diverse mechanisms to arrest cell cycle in G1  
408 phase or these diverse pathways could be due to the different cellular contexts used in the  
409 experiments. It is interesting to note that K-Rta mediated increase in p27 levels was not at the  
410 transcriptional level and was independent of K-Rta's transactivation ability. The transactivation  
411 function of several herpesviral immediate early genes including Zta, IE2 and ICP0 was found to  
412 be dispensable for cell cycle arrest (25, 45-47). Instead, the ability to arrest cell cycle was  
413 mapped to key motifs that are involved in protein-protein interactions like the bZIP domain of E-  
414 Zta and RING finger domain for ICP0 (25, 45). These studies suggest that the transactivation

415 function of immediate early genes may be less important for mediating cell cycle arrest than  
416 direct interactions with key cell cycle regulators.

417         In normal cells, p27 levels are maximal in quiescence but falls rapidly as the cells  
418 progress from G1 to S phase. p27 is a short-lived protein and its levels are mainly regulated by  
419 post-translational proteolytic degradation (39, 48). In the late G1 phase, degradation of p27 is  
420 mediated by SCF/Skp2 E3 ubiquitin ligase complex that requires phosphorylation of p27 at T187  
421 residue by cyclin E,A/ CDK2 complex (49). The phosphorylation at T187 creates a recognition  
422 site for Skp2 complex, which induces p27 poly-ubiquitination and subsequent degradation by the  
423 proteasome (41-43). The data presented here demonstrate that p27 was more stable in K-Rta  
424 expressing cells. This finding was also supported by decreased poly-ubiquitination of p27  
425 observed in K-Rta expressing cells. It is noteworthy that p27 degradation involves both Skp2-  
426 dependent and -independent proteosomal degradation pathways (39). We have focused on Skp2-  
427 dependent proteosomal pathway, as it is the best-characterized and most potent degradation  
428 pathway that determines p27 stability. It remains to be clarified whether K-Rta mediated  
429 stabilization of p27 also involve another degradation pathway besides Skp2-dependent pathway  
430 that would function independently of T187 phosphorylation.

431         Based on our results, we hypothesize that there are at least three non-mutually exclusive  
432 possibilities by which K-Rta can induce cell cycle arrest, as summarized in Figure 8. First, K-Rta  
433 may sequester p27 in the nucleus to prevent its export to the cytoplasm by direct or indirect  
434 interaction. The localization of p27 seems to be finely regulated during G1 progression (39). To  
435 act as a cell cycle inhibitor, p27 must be localized in the nucleus, whereas its cytoplasmic export  
436 allows cell cycle progression. In our study we observed the accumulation of p27 in the nucleus  
437 of K-Rta expressing cells, but it is difficult to resolve whether K-Rta is directly modulating the  
438 subcellular localization of p27 or the nuclear accumulation of p27 is an indirect consequence of

439 K-Rta mediated cell cycle arrest. The second possibility is that K-Rta may induce or repress the  
440 expression of any upstream kinase or phosphatase, which may regulate the phosphorylation of  
441 p27. Several key phosphorylation sites have been characterized in recent years including S10,  
442 T157 and T198 that determine p27 stability and subcellular localization (39). The third  
443 possibility is that K-Rta may directly or indirectly interact with SCF/Skp2 complex to disrupt the  
444 binding between p27 and Skp2, which targets p27 for subsequent proteosomal degradation. Since  
445 K-Rta has been shown to possess E3 ubiquitin ligase activity, the last scenario becomes  
446 particularly interesting if Skp2 is identified as a target for K-Rta-mediated proteosomal  
447 degradation (50). In that case p27 will escape Skp2 mediated proteosomal degradation and would  
448 accumulate in the nucleus. We were able to co-immunoprecipitate over expressed tagged  
449 versions of K-Rta and Skp2 in transiently transfected 293T cells (Data not shown), however our  
450 effort to detect this interaction in vivo under physiologically relevant conditions was  
451 unsuccessful. It is plausible that the interaction between K-Rta and Skp2 is transient in nature  
452 and/or very weak.

453         Recent research suggests that KSHV lytic reactivation is tightly linked to B-cell terminal  
454 differentiation (51). KSHV remains latent in a not very well characterized B-cell compartment  
455 until B cells differentiate into plasma cells. This terminal differentiation provides the  
456 physiological lytic switch through plasma cell transcription factor X box binding protein 1  
457 (XBP-1s). Thus, KSHV like EBV reactivates by exploiting the terminal differentiation pathway  
458 of latently infected B cells. In most cell lineages, final differentiation is associated with loss of  
459 proliferation and cell cycle arrest in G1 phase (52). During the differentiation process, the  
460 expression of various CDKIs including p27 is up regulated. Strong evidence for a role of p27 in  
461 differentiation programs comes from studies in mice lacking p27, which shows altered  
462 differentiation program in various tissues (53-55). It would be interesting to investigate whether

463 K-Rta mediated up-regulation of p27 following lytic reactivation also plays a role in  
464 differentiation of B cells besides cell cycle arrest.

465         An issue that remains to be resolved is the experimental validation of the hypothesis of  
466 the presumed benefit of cell cycle arrest during KSHV or in general herpesvirus lytic replication.  
467 Most studies including ours have investigated the role of herpesviral immediate early genes in  
468 cell cycle regulation in an over expressed system. Experimental validation in the context of  
469 normal viral infection setting proves to be a challenging endeavor, most likely because of  
470 temporal and ephemeral nature of cell cycle arrest. In case of KSHV, it has been shown that  
471 following K-Rta induction there is a substantial increase in the expression of vCyclin and LANA  
472 proteins, both of which have the potential to accelerate cell cycle progression modulating Rb-  
473 E2F pathway. Clearly, more work is needed to obtain a comprehensive understanding of cell  
474 cycle regulation in herpesvirus lytic replication.

475         In summary our results demonstrate that KSHV encoded K-Rta is another player besides  
476 K8 that participate in arresting host cells in G1 phase following viral reactivation. K-Rta  
477 mediated cell cycle arrest was associated with stabilization and increased nuclear accumulation  
478 of p27. Our study has revealed a discrete functional role for K-Rta in host cell cycle regulation,  
479 which is independent of its function as a major viral transcriptional factor.



480 Acknowledgements

481           This work was supported in part by the Public Health Service grants CA-75903, P20  
482 RR15635 and P30 GM103509 from the National Institutes of Health.

483           We would like to thank Dr. Levon Abrahamyan for his help with confocal microscopy  
484 and Danielle Shea for help with flow cytometry. We also thank Dr. J. U. Jung at the University  
485 of Southern California for providing RTA-inducible BJAB cell line, Dr Luwen Zhang at the  
486 University of Nebraska, Lincoln for DG75 and Cro6 cell lines and Dr. Izumiya at UC Davis for  
487 Rta polyclonal serum.

## 488 References

- 489 1. Mesri EA, Cesarman E, Boshoff C. 2010. Kaposi's sarcoma and its associated  
490 herpesvirus. *Nat Rev Cancer* 10:707-719.
- 491 2. Cesarman E, Chang Y, Moore PS, Said JW, Knowles DM. 1995. Kaposi's sarcoma-  
492 associated herpesvirus-like DNA sequences in AIDS-related body-cavity-based  
493 lymphomas. *N Engl J Med* 332:1186-1191.
- 494 3. Chang Y, Cesarman E, Pessin MS, Lee F, Culpepper J, Knowles DM, Moore PS.  
495 1994. Identification of herpesvirus-like DNA sequences in AIDS-associated Kaposi's  
496 sarcoma. *Science* 266:1865-1869.
- 497 4. Soulier J, Grollet L, Oksenhendler E, Cacoub P, Cazals-Hatem D, Babinet P,  
498 d'Agay MF, Clauvel JP, Raphael M, Degos L, Sigaux F. 1995. Kaposi's sarcoma-  
499 associated herpesvirus-like DNA sequences in multicentric Castlemans disease. *Blood*  
500 86:1276-1280.
- 501 5. Ganem D. 2010. KSHV and the pathogenesis of Kaposi sarcoma: listening to human  
502 biology and medicine. *J Clin Invest* 120:939-949.
- 503 6. Sun R, Lin SF, Gradoville L, Yuan Y, Zhu F, Miller G. 1998. A viral gene that  
504 activates lytic cycle expression of Kaposi's sarcoma-associated herpesvirus. *Proc Natl*  
505 *Acad Sci U S A* 95:10866-10871.
- 506 7. Lukac DM, Renne R, Kirshner JR, Ganem D. 1998. Reactivation of Kaposi's sarcoma-  
507 associated herpesvirus infection from latency by expression of the ORF 50 transactivator,  
508 a homolog of the EBV R protein. *Virology* 252:304-312.
- 509 8. Gradoville L, Gerlach J, Grogan E, Shedd D, Nikiforow S, Metroka C, Miller G.  
510 2000. Kaposi's sarcoma-associated herpesvirus open reading frame 50/Rta protein

- 511 activates the entire viral lytic cycle in the HH-B2 primary effusion lymphoma cell line. J  
 512 Virol 74:6207-6212.
- 513 9. Xu Y, AuCoin DP, Huete AR, Cei SA, Hanson LJ, Pari GS. 2005. A Kaposi's  
 514 sarcoma-associated herpesvirus/human herpesvirus 8 ORF50 deletion mutant is defective  
 515 for reactivation of latent virus and DNA replication. J Virol 79:3479-3487.
- 516 10. Duan W, Wang S, Liu S, Wood C. 2001. Characterization of Kaposi's sarcoma-  
 517 associated herpesvirus/human herpesvirus-8 ORF57 promoter. Arch Virol 146:403-413.
- 518 11. Deng H, Young A, Sun R. 2000. Auto-activation of the rta gene of human herpesvirus-  
 519 8/Kaposi's sarcoma-associated herpesvirus. J Gen Virol 81:3043-3048.
- 520 12. Deng H, Chu JT, Rettig MB, Martinez-Maza O, Sun R. 2002. Rta of the human  
 521 herpesvirus 8/Kaposi sarcoma-associated herpesvirus up-regulates human interleukin-6  
 522 gene expression. Blood 100:1919-1921.
- 523 13. Chen J, Ueda K, Sakakibara S, Okuno T, Yamanishi K. 2000. Transcriptional  
 524 regulation of the Kaposi's sarcoma-associated herpesvirus viral interferon regulatory  
 525 factor gene. J Virol 74:8623-8634.
- 526 14. Chang PJ, Shedd D, Gradoville L, Cho MS, Chen LW, Chang J, Miller G. 2002.  
 527 Open reading frame 50 protein of Kaposi's sarcoma-associated herpesvirus directly  
 528 activates the viral PAN and K12 genes by binding to related response elements. J Virol  
 529 76:3168-3178.
- 530 15. Bowser BS, Morris S, Song MJ, Sun R, Damania B. 2006. Characterization of  
 531 Kaposi's sarcoma-associated herpesvirus (KSHV) K1 promoter activation by Rta.  
 532 Virology 348:309-327.

- 533 16. Salvant BS, Fortunato EA, Spector DH. 1998. Cell cycle dysregulation by human  
534 cytomegalovirus: influence of the cell cycle phase at the time of infection and effects on  
535 cyclin transcription. *J Virol* 72:3729-3741.
- 536 17. Izumiya Y, Lin SF, Ellison TJ, Levy AM, Mayeur GL, Izumiya C, Kung HJ. 2003.  
537 Cell cycle regulation by Kaposi's sarcoma-associated herpesvirus K-bZIP: direct  
538 interaction with cyclin-CDK2 and induction of G1 growth arrest. *J Virol* 77:9652-9661.
- 539 18. Huang SY, Hsieh MJ, Chen CY, Chen YJ, Chen JY, Chen MR, Tsai CH, Lin SF,  
540 Hsu TY. 2012. Epstein-Barr virus Rta-mediated transactivation of p21 and 14-3-3sigma  
541 arrests cells at the G1/S transition by reducing cyclin E/CDK2 activity. *J Gen Virol*  
542 93:139-149.
- 543 19. Chen YL, Chen YJ, Tsai WH, Ko YC, Chen JY, Lin SF. 2009. The Epstein-Barr virus  
544 replication and transcription activator, Rta/BRLF1, induces cellular senescence in  
545 epithelial cells. *Cell Cycle* 8:58-65.
- 546 20. Flemington EK. 2001. Herpesvirus lytic replication and the cell cycle: arresting new  
547 developments. *J Virol* 75:4475-4481.
- 548 21. Nishioka WK, Welsh RM. 1994. Susceptibility to cytotoxic T lymphocyte-induced  
549 apoptosis is a function of the proliferative status of the target. *J Exp Med* 179:769-774.
- 550 22. Kawaguchi Y, Van Sant C, Roizman B. 1997. Herpes simplex virus 1 alpha regulatory  
551 protein ICP0 interacts with and stabilizes the cell cycle regulator cyclin D3. *J Virol*  
552 71:7328-7336.
- 553 23. Hobbs WE, 2nd, DeLuca NA. 1999. Perturbation of cell cycle progression and cellular  
554 gene expression as a function of herpes simplex virus ICP0. *J Virol* 73:8245-8255.

- 555 24. Rodriguez A, Jung EJ, Yin Q, Cayrol C, Flemington EK. 2001. Role of c-myc  
 556 regulation in Zta-mediated induction of the cyclin-dependent kinase inhibitors p21 and  
 557 p27 and cell growth arrest. *Virology* 284:159-169.
- 558 25. Cayrol C, Flemington EK. 1996. The Epstein-Barr virus bZIP transcription factor Zta  
 559 causes G0/G1 cell cycle arrest through induction of cyclin-dependent kinase inhibitors.  
 560 *EMBO J* 15:2748-2759.
- 561 26. Wu FY, Chen H, Wang SE, ApRhys CM, Liao G, Fujimuro M, Farrell CJ, Huang J,  
 562 Hayward SD, Hayward GS. 2003. CCAAT/enhancer binding protein alpha interacts  
 563 with ZTA and mediates ZTA-induced p21(CIP-1) accumulation and G(1) cell cycle arrest  
 564 during the Epstein-Barr virus lytic cycle. *J Virol* 77:1481-1500.
- 565 27. Wu FY, Wang SE, Tang QQ, Fujimuro M, Chiou CJ, Zheng Q, Chen H, Hayward  
 566 SD, Lane MD, Hayward GS. 2003. Cell cycle arrest by Kaposi's sarcoma-associated  
 567 herpesvirus replication-associated protein is mediated at both the transcriptional and  
 568 posttranslational levels by binding to CCAAT/enhancer-binding protein alpha and  
 569 p21(CIP-1). *J Virol* 77:8893-8914.
- 570 28. Nakamura H, Lu M, Gwack Y, Souvlis J, Zeichner SL, Jung JU. 2003. Global  
 571 changes in Kaposi's sarcoma-associated virus gene expression patterns following  
 572 expression of a tetracycline-inducible Rta transactivator. *J Virol* 77:4205-4220.
- 573 29. Trivedi P, Takazawa K, Zompetta C, Cuomo L, Anastasiadou E, Carbone A, Uccini  
 574 S, Belardelli F, Takada K, Frati L, Faggioni A. 2004. Infection of HHV-8+ primary  
 575 effusion lymphoma cells with a recombinant Epstein-Barr virus leads to restricted EBV  
 576 latency, altered phenotype, and increased tumorigenicity without affecting TCL1  
 577 expression. *Blood* 103:313-316.

- 578 30. Shao R, Guo X. 2004. Human microvascular endothelial cells immortalized with human  
 579 telomerase catalytic protein: a model for the study of in vitro angiogenesis. *Biochem*  
 580 *Biophys Res Commun* 321:788-794.
- 581 31. Wen HJ, Yang Z, Zhou Y, Wood C. 2010. Enhancement of autophagy during lytic  
 582 replication by the Kaposi's sarcoma-associated herpesvirus replication and transcription  
 583 activator. *J Virol* 84:7448-7458.
- 584 32. Riccardi C, Nicoletti I. 2006. Analysis of apoptosis by propidium iodide staining and  
 585 flow cytometry. *Nat Protoc* 1:1458-1461.
- 586 33. Livak KJ, Schmittgen TD. 2001. Analysis of relative gene expression data using real-  
 587 time quantitative PCR and the  $2(-\Delta\Delta C(T))$  Method. *Methods* 25:402-408.
- 588 34. Tiscornia G, Singer O, Verma IM. 2006. Production and purification of lentiviral  
 589 vectors. *Nat Protoc* 1:241-245.
- 590 35. Giacinti C, Giordano A. 2006. RB and cell cycle progression. *Oncogene* 25:5220-5227.
- 591 36. Resnitzky D, Hengst L, Reed SI. 1995. Cyclin A-associated kinase activity is rate  
 592 limiting for entrance into S phase and is negatively regulated in G1 by p27Kip1. *Mol Cell*  
 593 *Biol* 15:4347-4352.
- 594 37. Chang H, Gwack Y, Kingston D, Souvlis J, Liang X, Means RE, Cesarman E, Hutt-  
 595 Fletcher L, Jung JU. 2005. Activation of CD21 and CD23 gene expression by Kaposi's  
 596 sarcoma-associated herpesvirus RTA. *J Virol* 79:4651-4663.
- 597 38. Pagano M, Tam SW, Theodoras AM, Beer-Romero P, Del Sal G, Chau V, Yew PR,  
 598 Draetta GF, Rolfe M. 1995. Role of the ubiquitin-proteasome pathway in regulating  
 599 abundance of the cyclin-dependent kinase inhibitor p27. *Science* 269:682-685.
- 600 39. Susaki E, Nakayama KI. 2007. Multiple mechanisms for p27(Kip1) translocation and  
 601 degradation. *Cell Cycle* 6:3015-3020.

- 602 40. Reynisdottir I, Massague J. 1997. The subcellular locations of p15(Ink4b) and  
 603 p27(Kip1) coordinate their inhibitory interactions with cdk4 and cdk2. *Genes Dev*  
 604 11:492-503.
- 605 41. Carrano AC, Eytan E, Hershko A, Pagano M. 1999. SKP2 is required for ubiquitin-  
 606 mediated degradation of the CDK inhibitor p27. *Nat Cell Biol* 1:193-199.
- 607 42. Tsvetkov LM, Yeh KH, Lee SJ, Sun H, Zhang H. 1999. p27(Kip1) ubiquitination and  
 608 degradation is regulated by the SCF(Skp2) complex through phosphorylated Thr187 in  
 609 p27. *Curr Biol* 9:661-664.
- 610 43. Malek NP, Sundberg H, McGrew S, Nakayama K, Kyriakides TR, Roberts JM.  
 611 2001. A mouse knock-in model exposes sequential proteolytic pathways that regulate  
 612 p27Kip1 in G1 and S phase. *Nature* 413:323-327.
- 613 44. Nakayama K, Nagahama H, Minamishima YA, Miyake S, Ishida N, Hatakeyama S,  
 614 Kitagawa M, Iemura S, Natsume T, Nakayama KI. 2004. Skp2-mediated degradation  
 615 of p27 regulates progression into mitosis. *Dev Cell* 6:661-672.
- 616 45. Lomonte P, Everett RD. 1999. Herpes simplex virus type 1 immediate-early protein  
 617 Vmw110 inhibits progression of cells through mitosis and from G(1) into S phase of the  
 618 cell cycle. *J Virol* 73:9456-9467.
- 619 46. Rodriguez A, Armstrong M, Dwyer D, Flemington E. 1999. Genetic dissection of cell  
 620 growth arrest functions mediated by the Epstein-Barr virus lytic gene product, Zta. *J*  
 621 *Virol* 73:9029-9038.
- 622 47. Wiebusch L, Hagemeyer C. 1999. Human cytomegalovirus 86-kilodalton IE2 protein  
 623 blocks cell cycle progression in G(1). *J Virol* 73:9274-9283.
- 624 48. Vervoorts J, Luscher B. 2008. Post-translational regulation of the tumor suppressor  
 625 p27(KIP1). *Cell Mol Life Sci* 65:3255-3264.

- 626 49. Montagnoli A, Fiore F, Eytan E, Carrano AC, Draetta GF, Hershko A, Pagano M.  
627 1999. Ubiquitination of p27 is regulated by Cdk-dependent phosphorylation and trimeric  
628 complex formation. *Genes Dev* 13:1181-1189.
- 629 50. Yu Y, Wang SE, Hayward GS. 2005. The KSHV immediate-early transcription factor  
630 RTA encodes ubiquitin E3 ligase activity that targets IRF7 for proteasome-mediated  
631 degradation. *Immunity* 22:59-70.
- 632 51. Wilson SJ, Tsao EH, Webb BL, Ye H, Dalton-Griffin L, Tsantoulas C, Gale CV, Du  
633 MQ, Whitehouse A, Kellam P. 2007. X box binding protein XBP-1s transactivates the  
634 Kaposi's sarcoma-associated herpesvirus (KSHV) ORF50 promoter, linking plasma cell  
635 differentiation to KSHV reactivation from latency. *J Virol* 81:13578-13586.
- 636 52. Kaldis P, Richardson HE. 2012. When cell cycle meets development. *Development*  
637 139:225-230.
- 638 53. Durand B, Gao FB, Raff M. 1997. Accumulation of the cyclin-dependent kinase  
639 inhibitor p27/Kip1 and the timing of oligodendrocyte differentiation. *EMBO J* 16:306-  
640 317.
- 641 54. Kiyokawa H, Kineman RD, Manova-Todorova KO, Soares VC, Hoffman ES, Ono  
642 M, Khanam D, Hayday AC, Frohman LA, Koff A. 1996. Enhanced growth of mice  
643 lacking the cyclin-dependent kinase inhibitor function of p27(Kip1). *Cell* 85:721-732.
- 644 55. Nakayama K, Ishida N, Shirane M, Inomata A, Inoue T, Shishido N, Horii I, Loh  
645 DY. 1996. Mice lacking p27(Kip1) display increased body size, multiple organ  
646 hyperplasia, retinal dysplasia, and pituitary tumors. *Cell* 85:707-720.
- 647  
648  
649



650 Figure Legends

651 Figure 1. KSHV reactivation following TPA treatment arrests cells in G0/G1 phase:

652 Asynchronously growing exponential cultures of BC3 and Cro6 (KSHV positive) and DG75  
653 (KSHV negative) cells were treated with TPA (20 ng/ml). At the indicated times post-TPA  
654 treatment, the cells were fixed, stained with propidium iodide (PI) and analyzed by flow  
655 cytometry. Cell cycle phase distribution was determined using ModFit LT version 2.0 software.  
656 Cell cycle profiles presented here are representative of two independent experiments.

657 Figure 2. K-Rta arrests cells in G0/G1 phase: (A) Asynchronously growing exponential

658 cultures of control cell line (TRExBJAB) and Rta inducible BJAB cell line (TRExBJABRta)  
659 were synchronized by serum starvation for 24 hours. Growth arrested cells were stimulated with  
660 medium containing 10% serum and doxycycline (Dox). At the indicated times post-Dox  
661 treatment, the cells were fixed, stained with propidium iodide (PI) and analyzed by flow  
662 cytometry. Cell cycle phase distribution was determined using ModFit LT version 2.0 software.  
663 Data represents the mean of three independent experiments. Errors bars represent SD for  
664 triplicate samples. A significant increase in the number of cells stuck at G0/G1 phase was noted  
665 in TRExBJAB vs TRExBJABRta at 48 hrs ( $p=0.006$ ) and 72 hrs ( $p<0.001$ ) post-Dox treatment.

666 (B) Asynchronously growing exponential cultures of TREx293 Rta cells were treated with  
667 doxycycline. At 72 hrs post-Dox treatment, treated and untreated cells were fixed, stained with  
668 PI and cell cycle status was determined by flow cytometry as described above. A significant  
669 arrest in G1 phase was noted for Dox treated TREx293Rta cells at 72 hrs post Dox treatment  
670 compared to untreated cells ( $p<0.001$ ). Cell cycle profiles presented here are mean of three  
671 independent experiments. Errors bars represent SD for triplicate samples.

672 Figure 3. K-Rta expressing cells have increased levels of p27<sup>kip1</sup>: (A) Asynchronously

673 growing exponential cultures of control cell line (TRExBJAB) and Rta inducible BJAB cell line

674 (TRExBJABRta) were synchronized by serum starvation for 24 hours. Growth arrested cells  
675 were stimulated with medium containing 10% serum and doxycycline. Doxycycline treated or  
676 untreated TRExBJAB and TRExBJABRta cells were harvested and the expression kinetics of  
677 key cell cycle regulators were followed by immunoblotting at indicated times. GAPDH served as  
678 a loading control. The numbers below p27 band indicate the relative intensities of the p27 protein  
679 normalized to GAPDH protein. (B) Asynchronously growing DG75 (KSHV negative) and BC3  
680 (KSHV positive) cells were treated with TPA (20 ng/ml) for 24 and 48 hrs. The lysates were  
681 immunoblotted with antibodies as indicated. (C) DG75 and Vero cells were transiently  
682 transfected with either empty Flag vector or Flag Rta expression plasmid. Human Microvascular  
683 Endothelial Cells (HMVEC) cells were transduced with equal amounts of either control  
684 lentivirus or lentivirus expressing K-Rta. The cells were harvested after 36 hrs and the lysates  
685 were immunoblotted with antibodies as indicated. The values below the figure represent relative  
686 density of p27 bands normalized to that of GAPDH bands.

687 Figure 4. K-Rta does not affect p27 at the transcriptional level: (A) RNA was harvested  
688 from parallel samples collected at 0, 24, 48 and 72 hrs from doxycycline treated or untreated  
689 TRExBJAB and TRExBJABRta cells from the same experiment as described in Fig 2. The  
690 samples were subjected to quantitative real-time PCR analysis to detect the transcript levels of  
691 K-Rta, p27 and GAPDH. Each sample was tested in triplicate and representative data obtained  
692 from two independent experiments is shown. Relative gene expression was normalized to  
693 GAPDH expression and the fold change in the expression of each gene was calculated by using  
694 the delta-delta Ct method. (B) Schematic diagram depicting various domains of Rta protein.  
695  $5 \times 10^6$  293-T cells were transiently transfected with 4  $\mu$ g of either empty Flag vector, Flag vector  
696 expressing full length K-Rta (FL) or Flag vector expressing truncated K-Rta (1-527 AA). The  
697 cells were harvested 36 hrs post transfection and whole cell lysate was immunoblotted with anti-

698 Flag antibody, anti-p27 antibody and anti-GAPDH antibody. LZ – Leucine zipper, NLS –  
699 Nuclear localization signal.

700 Figure 5. K-Rta affects p27 protein stability: (A) Stability test: K-Rta inducible BJAB cell  
701 cultures (TRExBJABRta) were treated with 50 µg/ml cyclohexamide (CHX) in the absence or  
702 presence of doxycycline (Dox) for indicated lengths of time (In hours). Cell lysates were  
703 subjected to Western blot analysis with indicated antibodies. The relative band intensity of p27  
704 (normalized to GAPDH) was plotted with respect to time after CHX addition. Gel images  
705 presented here are representative of three independent experiments. (B) Doxycycline treated and  
706 untreated (for 48 hrs) TRExBJABRta cells were pretreated with proteasome inhibitor MG132  
707 (20 µM) before harvesting. Cell extracts were prepared under denaturing lysis conditions and  
708 p27 was immunoprecipitated (IP) from Dox treated and untreated TRExBJABRta cells.  
709 Immunoprecipitates were subjected to Western blot analysis using p27, Rta and GAPDH  
710 antibody. The same membrane was stripped and reprobed with anti-Ubiquitin (Ub) antibody. Gel  
711 images presented here are representative of three independent experiments. WB – Western Blot.

712 Figure 6. K-Rta can promote nuclear localization of p27: (A) TRExBJABRta cells were  
713 treated with doxycycline for 48 hrs. The Dox treated and untreated cells were fixed with 4%  
714 paraformaldehyde for 20 min, permeabilized with 0.2% Triton X-100 in PBS for 10 minutes, and  
715 blocked for 30 min with 2% bovine serum albumin (BSA) in PBS. After incubation with primary  
716 antibodies (anti-p27 and anti-Rta, both 1:250 dilution) in 2% BSA for 2 hrs at room temperature,  
717 the cells were incubated with anti-mouse Alexa-Fluor-488 and anti-rabbit Alexa-Fluor-647  
718 conjugated secondary antibodies (1:1000) for 1 hour at room temperature. The Rta and p27  
719 localization and DAPI stained nuclei were visualized by confocal microscopy. (B) Cytosolic and  
720 nuclear fractions were extracted from TRExBJABRta cells treated with doxycycline and subjected  
721 to western blotting with indicated antibodies. TATA binding protein (TBP) and  $\alpha$ -tubulin were

722 used as a nuclear fraction and cytosolic fraction loading control respectively. The bar graph on  
723 the right side shows percent of p27 quantitated in the nuclear fraction (normalized to total p27  
724 levels). Gel images presented here are representative of two independent experiments.

725 Figure 7. K-Rta expressing cells have decreased levels of Skp2: TRExBJABRta cells were  
726 serum starved for 24 hours. Growth arrested cells were stimulated with medium containing 10%  
727 serum and doxycycline. At times indicated doxycycline treated and untreated cells were  
728 harvested and lysates were subjected to immunoblot analysis with indicated antibodies. GAPDH  
729 served as a loading control. Gel images presented here are representative of two independent  
730 experiments.

731 Figure 8. Knock down of p27 expression by sh-RNAs attenuates K-Rta induced cell cycle  
732 arrest: The parent cell line, TRExBJABRta cells or TRExBJABRta cells stably expressing  
733 control sh-RNA (clone #1 and #2) or sh-RNA against p27 (clone #1 and #2) were serum starved  
734 for 24 hrs. Growth arrested cells were stimulated with medium containing 10% serum and  
735 doxycycline. At 48 hrs post doxycycline treatment, the cells were harvested for flow cytometry  
736 and immunoblot analysis. (A) Whole cell lysates were subjected to immunoblot analysis with  
737 indicated antibodies. GAPDH served as a loading control. The numbers below p27 band indicate  
738 the relative intensities of the p27 protein normalized to GAPDH protein. (B) For flow cytometry,  
739 the cells were fixed, stained with propidium iodide and cell cycle phase distribution was  
740 determined using ModFit LT version 2.0 software. Data represents the mean  $\pm$  SD of two  
741 independent experiments.

742 Figure 9. A schematic diagram for K-Rta mediated cell cycle arrest in G0/G1 phase: 1, 2  
743 and 3 represent alternate possibilities elaborated in the discussion section by which K-Rta can  
744 induce cell cycle arrest.

Figure 1.

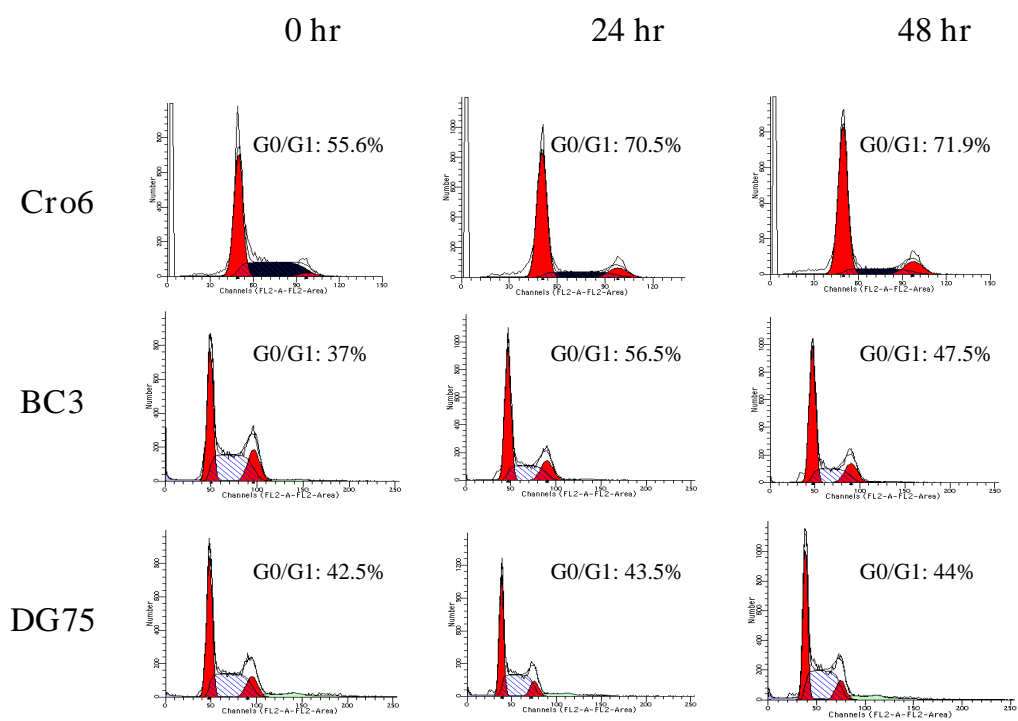
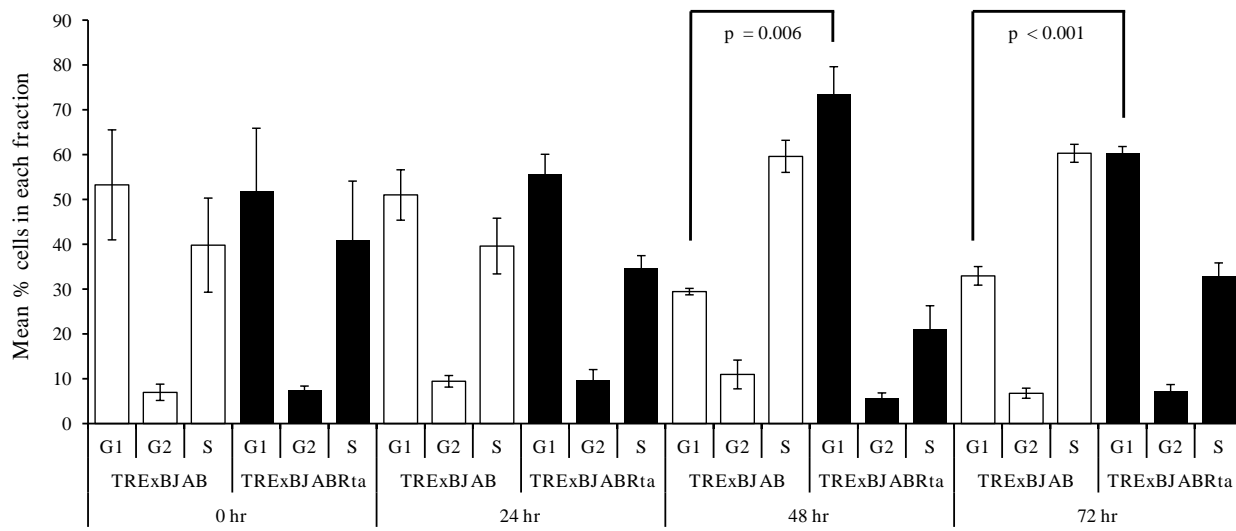


Figure 2.

A



B

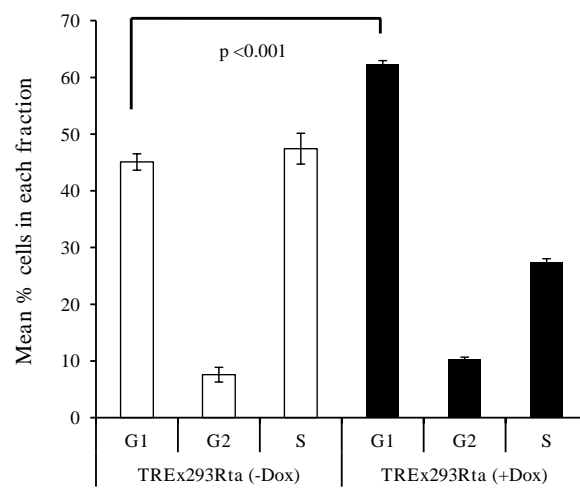
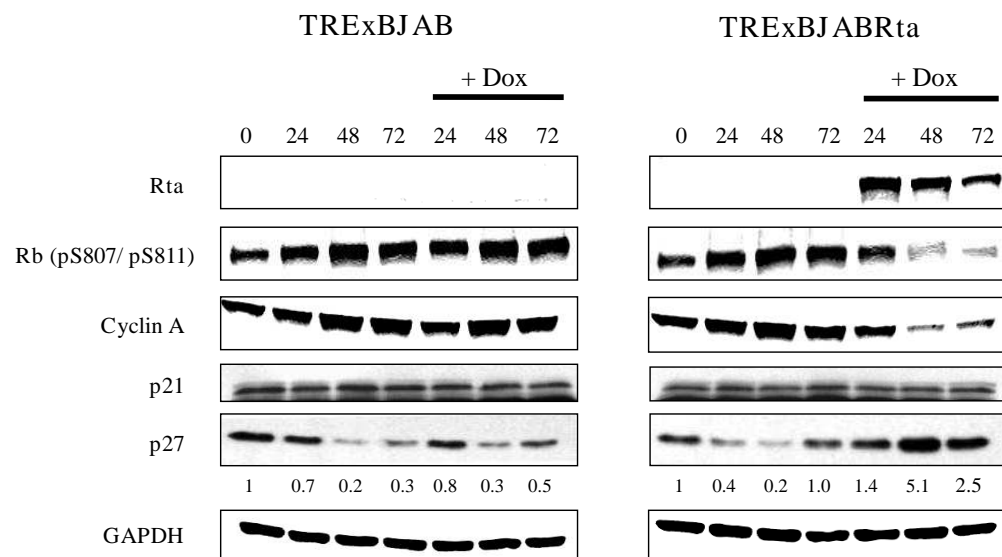


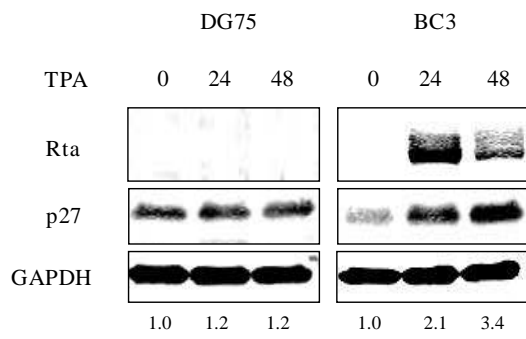
Figure 3.

A





**B**



**C**

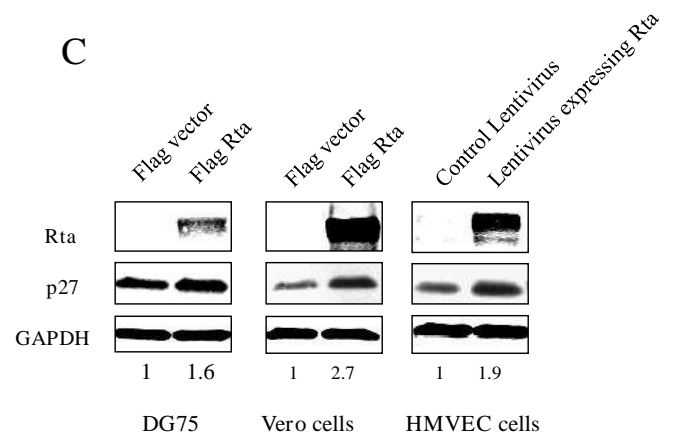
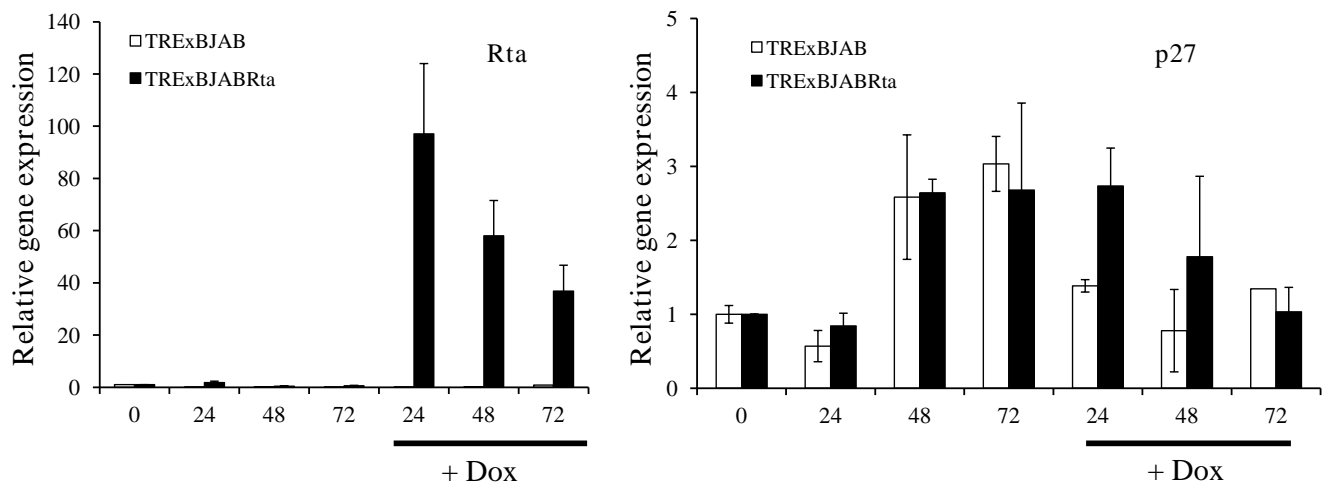


Figure 4.

A



B

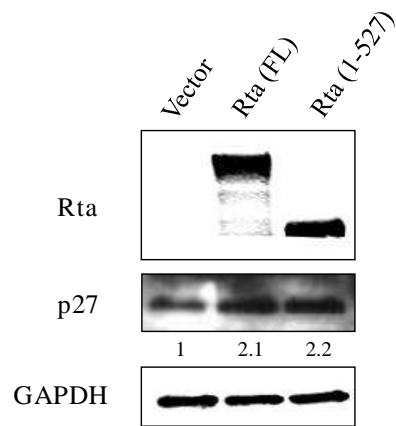
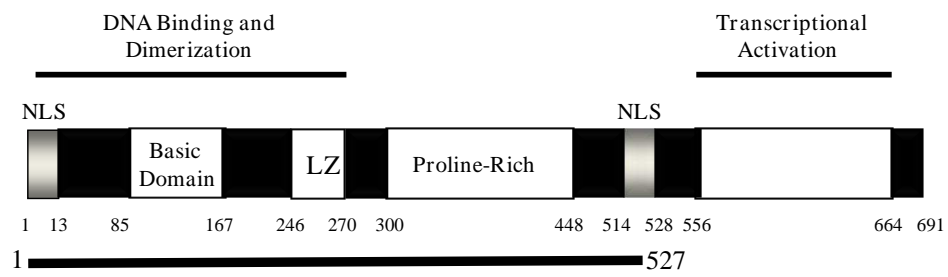


Figure 5.

A

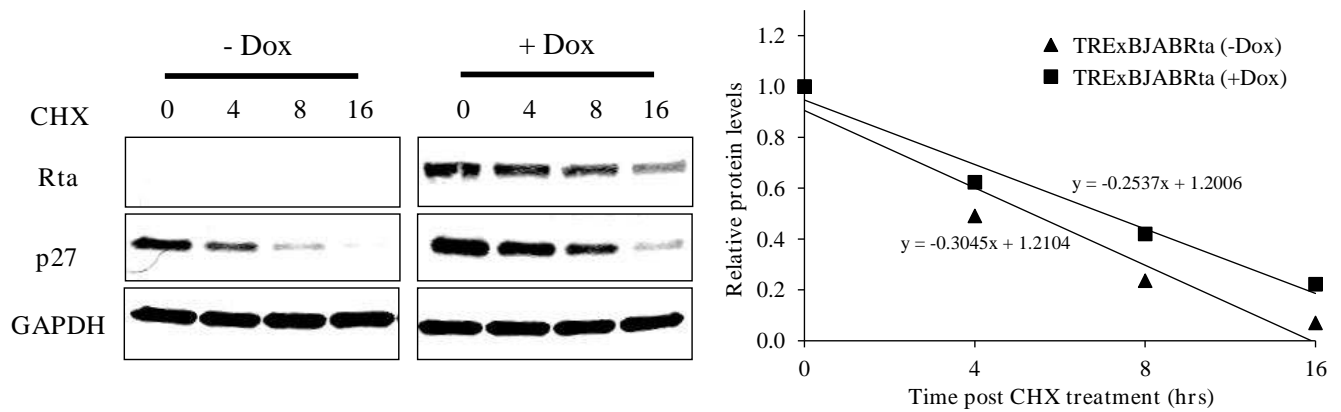
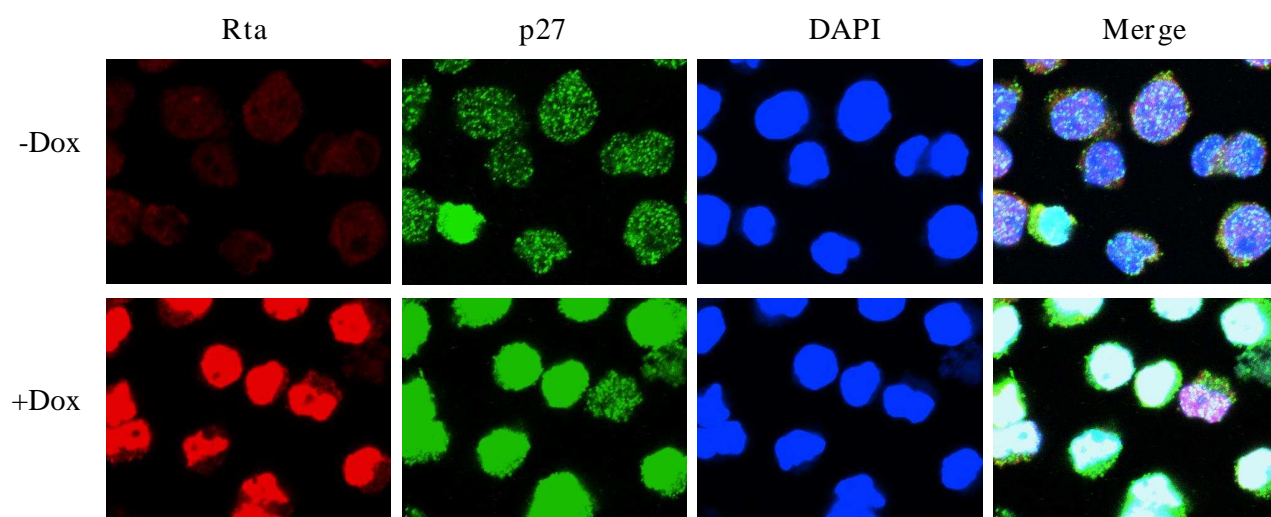




Figure 6.

A



B

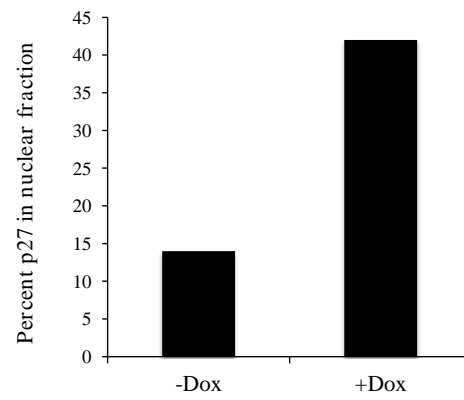
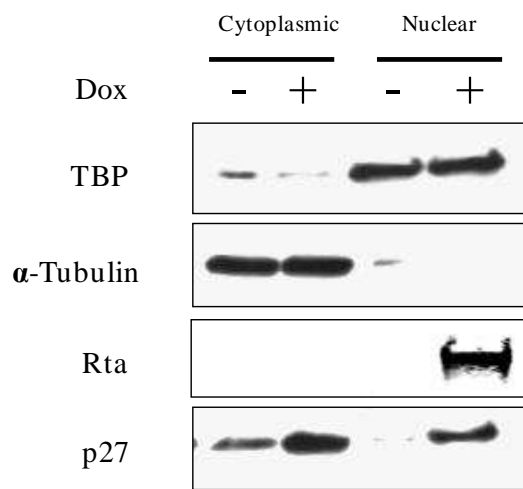


Figure 7.

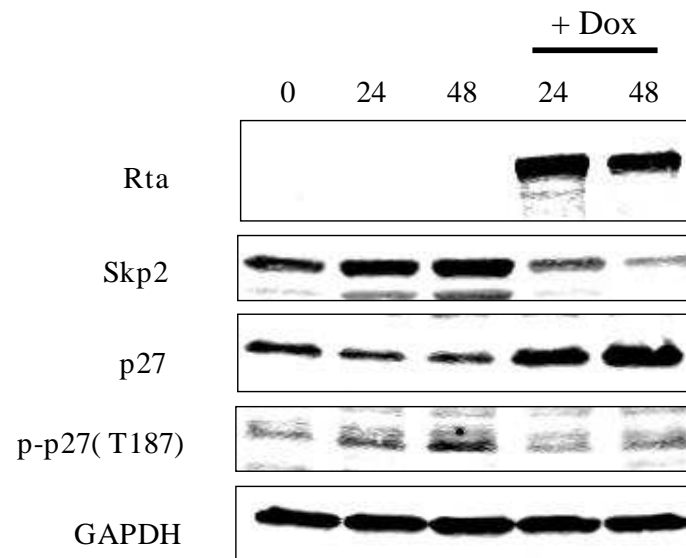
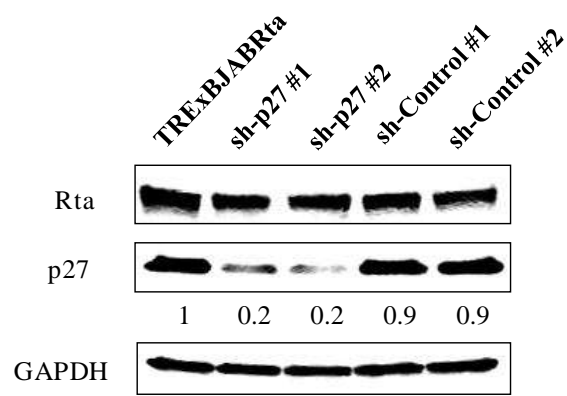




Figure 8.

A



B

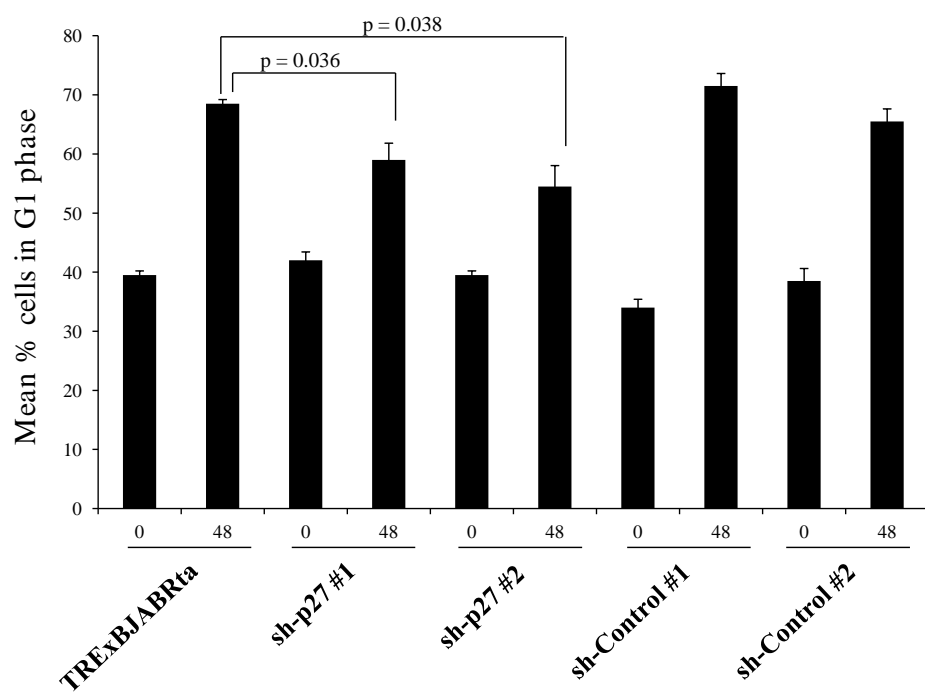


Figure 9.

